ORIGINAL ARTICLE

Korean J Intern Med 2021;36(Suppl 1):S180-S195
https://doi.org/10.3904/kjim.2019.413

L-carnitine treatment attenuates renal tubulointerstitial fibrosis induced by unilateral ureteral obstruction

Hai Yan Zhao[1,2,3], Hui Ying Li[1,3], Jian Jin[1], Ji Zhe Jin[1], Long Ye Zhang[1], Mei Ying Xuan[2], Xue Mei Jin[4], Yu Ji Jiang[1], Hai Lan Zheng[1], Ying Shun Jin[1], Yong Jie Jin[5], Bum Soon Choi[5], Chul Woo Yang[5], Shang Guo Piao[1], and Can Li[1]

[1]Department of Nephrology, [2]Health Examination Center, [3]Postdoctoral Research Institute, [4]Department of Pathology, Yanbian University Hospital, Yanji, China; [5]Department of Internal Medicine, College of Medicine, The Catholic University of Korea, Seoul, Korea

Received: December 3, 2019
Revised : January 22, 2020
Accepted: February 5, 2020

Correspondence to
Shang Guo Piao, M.D.
Department of Nephrology, Yanbian University Hospital, #1327 Juzi St., Yanji 133000, China
Tel: +86-155-2677-0987
Fax: +86-433-251-3610
E-mail: piaoshangguo@163.com
https://orcid.org/0000-0003-0230-3243

Background/Aims: Accumulating evidence indicates that L-carnitine (LC) protects against multiorgan damage through its antioxidant properties and preservation of the mitochondria. Little information is available about the effects of LC on renal fibrosis. This study examined whether LC treatment would provide renoprotection in a rat model of unilateral ureteral obstruction (UUO) and *in vitro*.

Methods: Sprague-Dawley rats that underwent UUO were treated daily with LC for 7 or 14 days. The influence of LC on renal injury caused by UUO was evaluated by histopathology, and analysis of gene expression, oxidative stress, mitochondrial function, programmed cell death, and phosphatidylinositol 3-kinase (PI3K)/AKT/forkhead box protein O 1a (FoxO1a) signaling. In addition, H_2O_2-exposed human kidney cells (HK-2) were treated with LC.

Results: LC treatment inhibited expression of proinflammatory and profibrotic cytokines, and was followed by a significant attenuation of tubulointerstitial inflammation and fibrosis. The increased oxidative stress caused by UUO was associated with mitochondrial dysfunction and excessive apoptosis and autophagy via PI3K/AKT/FoxO1a-dependent signaling, and this was abrogated by administration of LC. In H_2O_2-exposed HK-2 cells, LC decreased intracellular production of reactive oxygen species, and suppressed expression of profibrotic cytokines and reduced the number of apoptotic cells.

Conclusions: LC protects against the progression of tubulointerstitial fibrosis in an obstructed kidney.

Keywords: L-carnitine; Unilateral ureteral obstruction; Oxidative stress; Autophagy; Mitochondria

INTRODUCTION

Chronic kidney disease (CKD) is a major human health problem worldwide. The United States Renal Data Service annual reports indicate that the overall prevalence of CKD in the general population is up to 14% and that it is increasing annually [1]. Progression of CKD to end-stage renal disease (ESRD) requires costly renal replacement therapy. Therefore, minimizing this clinical dilemma may improve the quality of life of people with CKD and reduce the economic burden on society. Renal tubulointerstitial fibrosis (TIF) is the final common end-

pISSN 1226-3303
eISSN 2005-6648
http://www.kjim.org

ing and histological feature of CKD that leads to ESRD. Unilateral ureteral obstruction (UUO) is a reproducible rodent experimental model of TIF, characterized by interstitial inflammation, overproduction of extracellular matrix, tubular dilatation, atrophy, and fibrosis. The molecular mechanisms underlying renal TIF are multifactorial. Studies have suggested that upregulation of the profibrotic cytokine transforming growth factor-β1 (TGF-β1) and inflammatory mediators, oxidative stress, and programmed cell death (apoptosis and autophagy) play important roles [2,3].

L-carnitine (LC, L-β-hydroxy-γ-N-trimethylaminobutyric acid), a quaternary ammonium compound, primarily acts as an essential cofactor for the β-oxidation of fatty acids by promoting the transport of long-chain fatty acids across the mitochondrial membrane in the form of acyl carnitine esters. The products of the β-oxidation (two carbon molecules) are then used by the Krebs cycle to produce adenosine triphosphate as a form of stored energy. Therefore, LC inhibits free radical generation, which contributes to the maintenance of fatty acid β-oxidation in mitochondria and protects tissues from damage by renewal of oxidized membrane lipids [4]. Moreover, LC has been considered to be a direct scavenger of O_2- and H_2O_2. Therefore, LC may possess antioxidant properties beyond its action on lipid metabolism. There is overwhelming evidence that LC confers benefits in diabetic podocyte injury [5] and myocardial infarction [6]. We have demonstrated that LC treatment ameliorates cyclosporine-induced pancreatic and renal injury [7]. Similar nephroprotection by LC is also seen in ischemia-reperfusion [8], contrast-induced nephropathy [9], hypertension-associated renal fibrosis [10], cisplatin nephropathy [11], and nephrotic syndrome [12].

In this context, we hypothesized that LC may protect against UUO-induced TIF. To test this hypothesis, we studied the effects of LC by measuring oxidative stress, mitochondrial function, programmed cell death, and phosphatidylinositol 3-kinase (PI3K)/AKT/forkhead box protein O 1a (FoxO1a) signaling in a well-known rat model of UUO and in H_2O_2-treated HK-2 cell lines.

METHODS

Establishment of UUO model and treatment schedule

All animal care and experimental procedures in this study were reviewed and approved by the Animal Experimentation Ethics Committee of Yanbian University Health Science Center (YBU-2017-2-3). Following acclimatization for 1 week, weight-matched male Sprague-Dawley rats weighing 220 to 240 g were housed in individual cases with a 12-hour artificial light-dark cycle and permitted free access to standard chow and water. The rats were randomly assigned to five groups: Sham operation (Sham, n = 6); UUO 7 days (UUO7; n = 8); UUO + LC7 (n = 8); UUO 14 days (UUO14; n = 8); and UUO + LC14 (n = 8). Induction of UUO was performed as described previously [13]. Briefly, rats were anesthetized with pentobarbital (40 mg/kg) and a flank incision was made. After exposure of the kidneys and ureters, the left ureter was ligated with 4-0 silk, followed by suture of the incision. Sham operation was performed similarly, but without ligation of the left ureter. Administration of LC (200 mg/kg/day intraperitoneal) was started 24 hours later and continued for 14 days, and sham-operated rats were injected intraperitoneally with sterile saline at a dose of 1 mg/mL/day. After 7 or 14 days of treatment, rats were euthanized and the obstructed kidneys were rapidly harvested for further examination.

LC (Sigma Aldrich C0158) was diluted in sterile saline to a final concentration of 200 mg/mL. The dose of LC treatment used in this study was chosen based on that used in previous study [14].

Measurement of renal function

Renal function, including serum creatinine (Scr), blood urea nitrogen (BUN), and cystatin C (CysC), was measured by a quantitative enzyme colorimetric method (Roche Cobas 8000 Core ISE, Roche Diagnostics, Mannheim, Germany).

Antibodies

The antibodies used in this study for immunohistochemistry and immunoblotting were as follows: ectodermal dysplasia 1 (ED-1, Serotec Inc., Oxford, UK), osteopontin (OPN, #ab8448, Abcam, Cambridge, UK), transforming growth factor-β1 (TGF-β1, R&D Systems, Minneapolis, MN, USA), connective-tissue growth factor

(CTGF, #ab125943, Abcam), matrix metalloproteinase-2 (MMP-2, #ab38929, Abcam), macrophage chemotactic protein-1 (MCP-1, Santa Cruz Biotechnoogy Inc., Santa Cruz, CA, USA), toll-like receptor-2 (TLR-2, Santa Cruz Biotechnoogy Inc.), heme-oxygenase-1 (HO-1, #ab13248, Abcam), superoxide dismutase-1 (SOD1, #ab16831, Abcam), superoxide dismutase-2 (SOD2, #ab13534, Abcam), nicotinamide adenine dinucleotide phosphate oxidase 2 (NOX-2, #ab31092, Abcam), nicotinamide adenine dinucleotide phosphate oxidase 4 (NOX-4, #ab109225, Abcam), translocase of the outer mitochondrial membrane 20 (TOMM20, #ab186734, Abcam), nicotinamide adenine dinucleotide dehydrogenase (ubiquinone) 1 alpha subcomplex 10 (NDUFA10, #ab96464, Abcam), succinate dehydrogenase complex subunit A (SDHA, #ab66484, Abcam), dynamin-related protein 1 (DLP1/Drp1, BD Transduction Laboratories, Lexington, KY, USA), optic atrophy protein 1 (OPA1, #ab90857, Abcam), B-cell lymphoma-2 (Bcl-2, #ab59348, Abcam), Bcl2-associated X (Bax, #ab32503, Abcam), cleaved caspase-3 (Millipore, Billerica, MA, USA), LC3B (#ab192890, Abcam), Beclin-1 (#ab62557, Abcam), P62 (#ab56416, Abcam), PI3K (#ab180967, Abcam), AKT (protein kinase B, #ab8805, Abcam), phospho-AKT (#ab38449, Abcam), FoxO1a (#ab70382, Abcam), phospho-FoxO1a (#ab131339, Abcam), α-smooth muscle actin (α-SMA, #ab5694, Abcam), β-actin (#ab8226, Abcam).

Histopathology

Harvested kidney specimens were rapidly fixed in periodate-lysine-paraformaldehyde solution and embedded in wax. Following dewaxing, 4-μm sections were conducted and stained with Masson's trichrome and hematoxylin. The quantitative analysis of TIF was performed using a color image auto-analyzer (TDI Scope Eye Version 3.6 for Windows, Olympus, Seoul, Korea). A minimum of 20 fields per section was evaluated by counting the percentage of injured area under × 100 magnification. Histopathological analysis was fulfilled in randomly selected cortical fields of sections by a pathologist blinded to the assignment of the treatment groups.

Immunohistochemistry

Immunohistochemistry was performed as described previously [7]. Twenty different fields in each section at × 400 magnification were analyzed using a color image analyzer (TDI Scope Eye Version 3.0 for Windows, Olympus, Tokyo, Japan).

Transmission electron microscopy

The procedure of transmission electron microscopy was performed as we previously detailed [15]. Kidney tissues were post-fixed with 1% osmium oxide (OsO_4) and embedded in Epon 812 following fixation in 2.5% glutaraldehyde in 0.1 M phosphate buffer. Ultrathin sections were cut and stained with uranyl acetate/lead citrate, and photographed with a JEM-1200EX transmission electron microscope (JEOL Ltd., Tokyo, Japan). Using an autoimage analyzer, the number and size of mitochondria were measured in 20 random unoverlapped proximal tubular cells (TDI Scope Eye Version 3.0 for Windows, Olympus, Tokyo, Japan).

Immunoblotting

Immunoblotting was performed as described previously [7]. Appropriate kidney specimens were selected to perform immunoblotting analysis according to protein loading lines as follows: sham (n = 6); UUO7 (n = 7); UUO + LC (n = 7); UUO14 (n = 8); UUO + LC14 (n = 8). Images were analyzed with an image analyzer (Quantity One, Bio-Rad Tachnical Service Department, Hercules, CA, USA). Optical densities were obtained using the sham group as 100% reference and normalized with β-actin.

In situ TUNEL assay

Apoptosis in tissue sections was identified using the ApopTag *in situ* Apoptosis Detection Kit (Sigma-Aldrich, Millipore). The number of terminal deoxynucleotidyl transferase dUTP nick end labeling (TUNEL)-positive cells was counted on 20 different fields in each section at × 400 magnification.

Enzyme-linked immunosorbent assay

A twenty-four-hour urine for each rat was collected and centrifuged. The supernatants were applied to determine the concentrations of the DNA adduct 8-hydroxy-2′-deoxyguanosine (8-OHdG) using a competitive enzyme-linked immunesorbent assay (Japan Institute for the Control of Aging, Shizuoka, Japan) according to the manufacturer's instruction. All samples were performed in triplicate and averaged.

https://doi.org/10.3904/kjim.2019.413

Cell culture and treatment

HK-2 cells from an immortalized human proximal tubular epithelial cell line were grown in Dulbecco's modified Eagle's medium/Nutrient F12 (DMEM/F12; HyClone, GE Healthcare Life Science, Logan, UT, USA) supplemented with 10% fetal bovine serum (FBS; Gibco, Thermo Fisher Scientific Inc., Waltham, MA, USA), 100 U/mL penicillin, and 100 μg/mL streptomycin (Gibco; Thermo Fisher Scientific Inc.). The cells were cultured in a humidified incubator with 5% CO_2 at 37°C. For some experiments, cells were pretreated with different concentrations of LC (10 or 100 μM) for 1 hour, and then treated with H_2O_2 (500 μM) with or without treatment with LC for 24 hours.

Cell viability assay

HK-2 cell viability was examined using cell counting kit-8 (CCK-8; Dojindo, Kumamoto, Japan) according to the manufacture's instructions. Approximately 1.0×10^4 cells/well were seeded in a 96-well plate. After treatment with H_2O_2 and/or LC, 10 μL of CCK-8 solution were added to each well and incubated at 37°C for 3 hours. Absorbance was measured as the optical density at 450 nm (VersaMax Microplate Reader, Molecular Devices, LLC, Sunnyvale, CA, USA).

Measurement of ROS production

The levels of intracellular reactive oxygen species (ROS) were measured using 2′,7′-dichlorodihydrofluorescein diacetate (H2-DCFDA, Invitrogen, Carlsbad, CA, USA) according to the manufacture's instructions. HK-2 cells were seeded at a density of 2.0×10^5 cells/well in a 6-well plate. After treatment with H_2O_2 or LC for the indicated time, cells were washed with phosphate-buffered saline and then incubated with H2-DCFDA for 30 minutes. Fluorescence was measured using a FACSCalibur flow cytometer (BD Biosciences, San Jose, CA, USA).

Apoptosis assay

Annexin V-positive HK-2 cells were detected using Annexin V-FITC apoptosis detection kit (Biosharp, Hefei, China) according to the manufacturer's protocol. Briefly, HK-2 cells were seeded and incubated with 500 μM H_2O_2 with or without LC (100 μM) for 24 hours, and the samples were analyzed using a FACSCalibur flow cytometer (BD Biosciences). Apoptotic cells were examined as a percentage of the total cell count. The percentage of apoptotic cells was calculated as the number of propidium iodide (PI)-positive and Annexin-V positive cells divided by the total number of cells. Three independent experiments were performed.

Statistical analysis

Data are presented as mean ± SEM. Multiple comparisons between groups were conducted using one-way analysis of variance and the Bonferroni post hoc test using SPSS software version 21.0 (IBM, Armonk, NY, USA). Statistical significance was accepted at $p < 0.05$.

RESULTS

Effect of LC on renal function

Table 1 summarizes the renal function in each of the treatment groups. Neither UUO nor LC influenced renal function, as shown by Scr, BUN, and CysC.

LC decreases UUO-induced tubulointerstitial fibrosis

Gross examination of the kidneys 7 days after UUO indicated kidney enlargement, hydronephrosis, ureterectasis, and a significant thinning of the renal cortex, changes that had developed further by day 14 (Fig. 1A).

Table 1. Renal function in the experimental groups

Parameter	Sham (n = 6)	UUO7 (n = 8)	UUO + LC7 (n = 8)	UUO14 (n = 8)	UUO + LC14 (n = 8)
Scr, mg/dL	0.28 ± 0.07	0.27 ± 0.04	0.26 ± 0.05	0.30 ± 0.07	0.31 ± 0.05
BUN, mg/dL	103.68 ± 11.39	106.51 ± 7.99	106.31 ± 9.36	114.94 ± 12.42	109.11 ± 7.03
CysC, mg/L	2.50 ± 0.17	2.61 ± 0.20	2.70 ± 0.31	2.72 ± 0.22	2.66 ± 0.25

Values are presented as mean ± SEM.
Sham, sham operation; UUO, unilateral ureteral obstruction; LC, L-carnitine; Scr, serum creatinine; BUN, blood urea nitrogen; CysC, cystatin C.

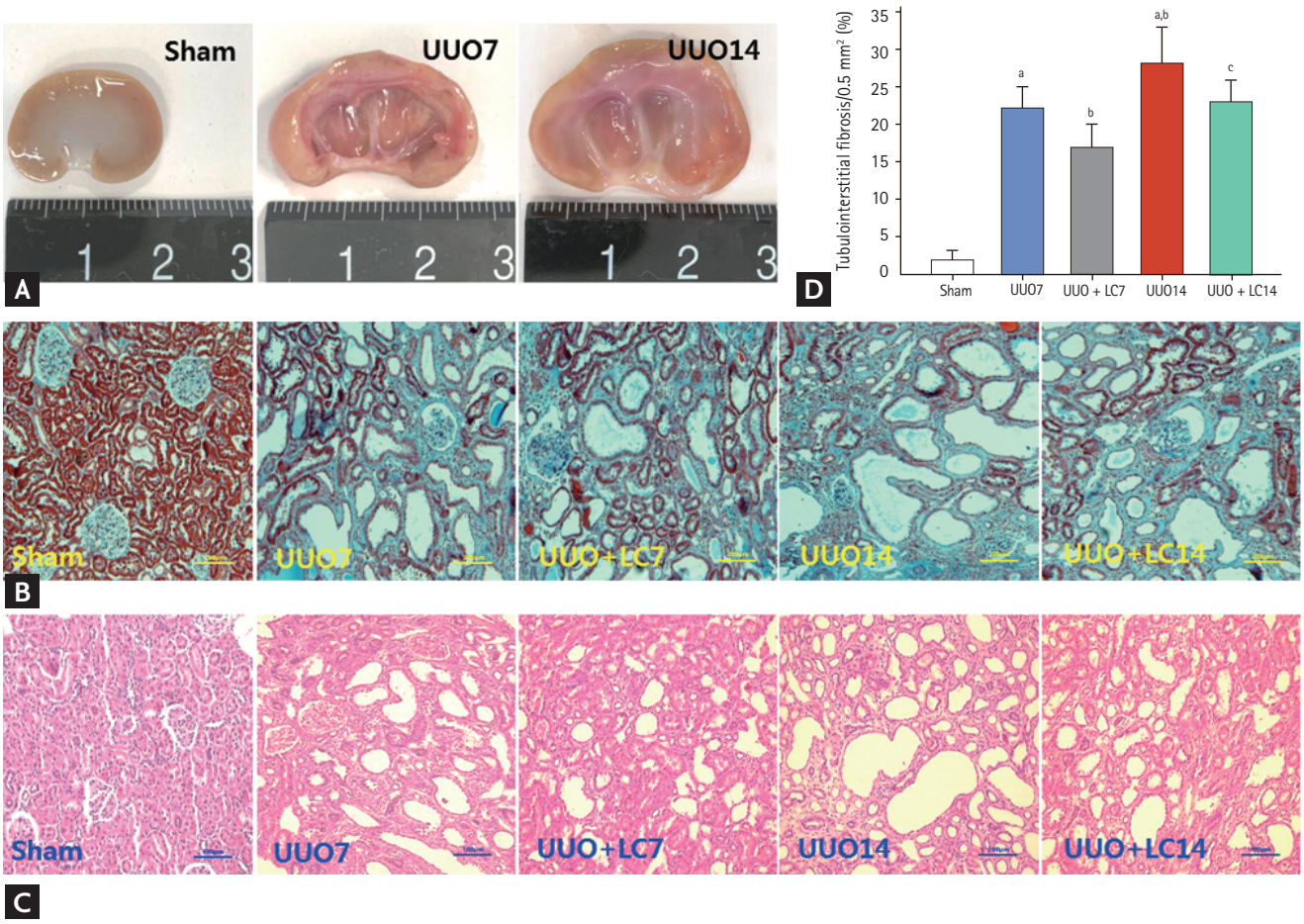

Figure 1. Representative photographs of gross findings (A) and photomicrographs of Masson trichrome (B) and hematoxylin-eosin staining (C), and quantitative analysis (D). UUO, unilateral ureteral obstruction; LC, L-carnitine. [a]$p < 0.01$ vs. sham, [b]$p < 0.05$ vs. UUO7, [c]$p < 0.05$ vs. UUO14.

Trichrome and hematoxylin-eosin staining demonstrated that rats that had undergone UUO displayed tubular basement membrane thickening, necrosis, vacuolization and atrophy (Fig. 1B and 1C), swelling of the tubular epithelium and interstitium, inflammatory cell infiltration, and mild TIF formation at day 7. After 14 days of UUO, renal histopathology was characterized by extensive tubular vacuolization and atrophy, a massive inflammatory cell influx, and moderate-to-severe TIF (Fig. 2). The sites of severe TIF were notably surrounded by areas of tubular vacuolization and atrophy (Fig. 1B, 1C and Fig. 3B, 3C). As evaluated with our quantitative analysis system, UUO induced a gradual increase in TIF at days 7 (22.10% ± 3.83%/0.5 mm² vs. 2.14% ± 0.95%/0.5 mm², $p < 0.01$) and 14 (28.47% ± 5.69%/0.5 mm² vs. 2.14% ± 0.95%/0.5 mm², $p < 0.01$) compared with sham operation, whereas LC treatment decreased TIF formation at both time points compared with UUO alone (17.62% ± 4.98%/0.5 mm² vs. UUO7, $p < 0.01$; 23.39% ± 3.71%/0.5 mm² vs. UUO14, $p < 0.05$) (Fig. 1D). At a molecular level, UUO significantly upregulated TGF-β1 and connective-tissue growth factor (CTGF) expression and induced MMP-2 overexpression at day 7 and this upregulation increased at day 14. All changes were reversed by administration of LC (Fig. 4).

LC decreases UUO-induced tubulointerstitial inflammation

Inflammation plays an important role in the renal fibrosis induced by UUO [16,17]. To address the effect of LC on inflammation, we evaluated inflammatory mediators by immunohistochemistry and immunoblotting.

https://doi.org/10.3904/kjim.2019.413

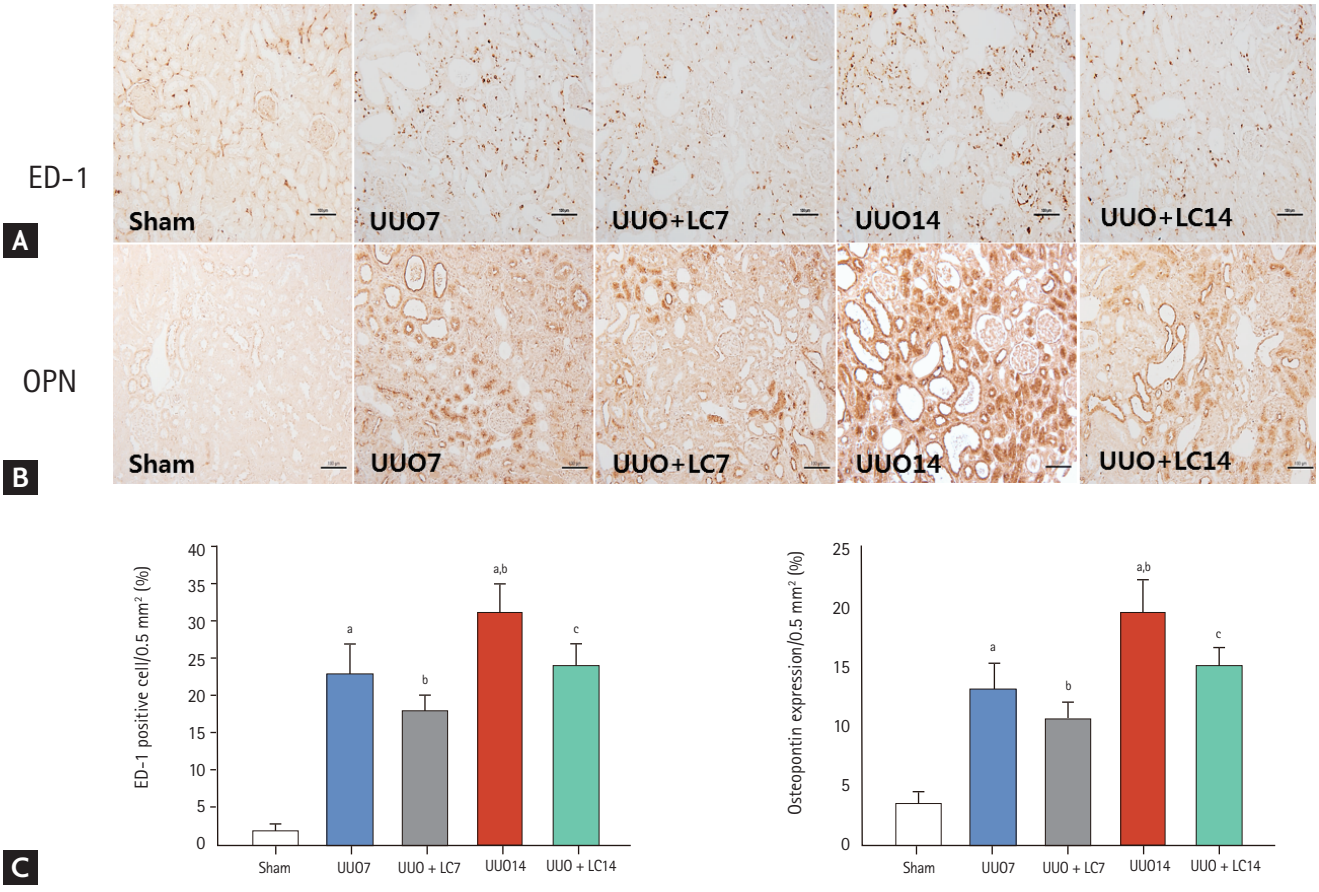

Figure 2. Representative photomicrographs of immunohistochemistry for ectodermal dysplasia 1 (ED-1) (A) or osteopontin (OPN) (B) and quantitative analyses (C). UUO, unilateral ureteral obstruction; LC, L-carnitine. [a]$p < 0.01$ vs. sham, [b]$p < 0.05$ vs. UUO7, [c]$p < 0.05$ vs. UUO14.

As shown in Figs. 2 and 3, constitutive expression of ED-1 and OPN in sham-operated kidneys was low, but was clearly increased in the obstructed kidneys at day 7 (ED-1: 23.44 ± 4.97/0.5 mm² vs. 2.15 ± 0.84/0.5 mm², $p < 0.01$; OPN: 13.24 ± 2.23/0.5 mm² vs. 3.41 ± 1.17/0.5 mm², $p < 0.01$), and was further increased at day 14 (ED-1: 31.63 ± 4.68/0.5 mm² vs. 23.44 ± 4.97/0.5 mm², $p < 0.01$; OPN: 19.63 ± 2.67/0.5 mm² vs. 13.24 ± 2.23/0.5 mm², $p < 0.01$). Immunoblotting showed that UUO caused a significant upregulation of macrophage chemotactic protein-1 (MCP-1) and toll-like receptor-2 (TLR-2) expression at day 7, and further upregulation was observed at day 14 (Fig. 4). Overexpression of these inflammatory mediators was markedly decreased by LC treatment.

LC decreases UUO-induced oxidative stress

Oxidative stress caused by UUO is well known to be closely associated with dysregulation of oxidant and antioxidant enzymes. In this study, immunoblotting revealed that LC treatment counteracted oxidative stress injury by upregulating SOD1 and SOD2 expression but downregulating NAPDH oxidase (NOX)-2 and NOX-4 compared with UUO alone (Fig. 5). Interestingly, UUO increased hemoxygenase (HO)-1 protein expression, and this was further increased following LC administration. This is consistent with previous reports by Chen et al. [18] and Qiao et al. [19] suggesting that induction of HO-1 is an adaptive response to UUO injury and that a further increase in HO-1 expression induced by LC plays a protective role. In addition, LC reduced 8-OHdG concentrations in serum (UUO7 + LC vs. UUO7: 46.14 ± 3.39 ng/mL vs. 60.12 ± 7.32 ng/mL; UUO14 + LC vs. UUO14: 50.52 ± 5.19 ng/mL vs. 71.16 ± 8.35 ng/mL, $p < 0.05$, respectively) (Fig. 6A) and urine (UUO7 + LC vs. UUO7:

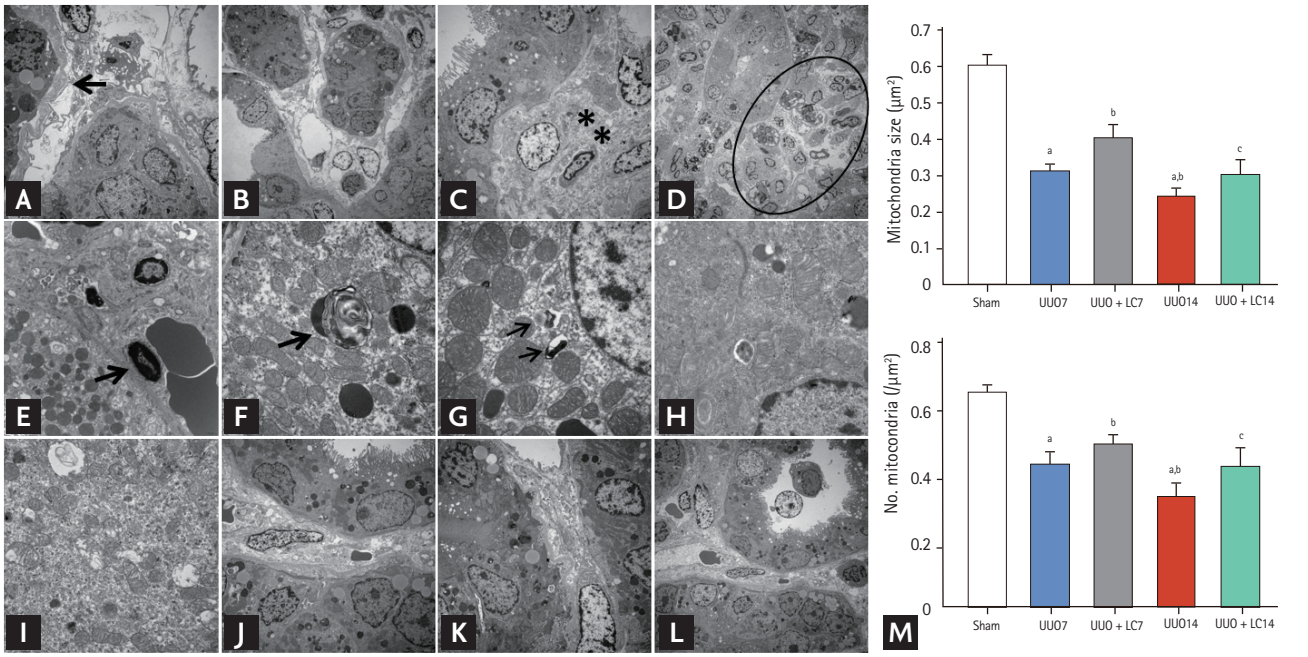

Figure 3. Representative photomicrographs of transmission electron microscopy illustrating the characteristics of renal injury in unilateral ureteral obstruction (UUO) with or without L-carnitine (LC) treatment and quantificative analyses of mitochondrial number and size. (A) Tubular basement membrane thickening (arrow) and interstitial collagen deposition; (B) tubular vacuolization and atrophy; (C) collagen fibers within tubulointerstitium (starlikes); (D) swelling of the tubular epithelium and interstitium, with massive inflammatory cell infiltration (circle); (E) apoptotic bodies (arrow); (F) myelin body (arrow); (G) autophagosome (arrows); (H) mitochondrial fission; (I) mitochondrial fussion; (J) mild tubular basement membrane thickening after LC treatment; (K) improved collagen deposition within the tubulointerstitium by LC; (L) LC treatment decreases the UUO-induced inflammatory cells infiltration within the tubulointerstitium. (M) Quantitative analyses of mitochondrial area and the number of mitochondria. [a]$p < 0.01$ vs. sham, [b]$p < 0.05$ vs. UUO, [c]$p < 0.05$ vs. UUO14.

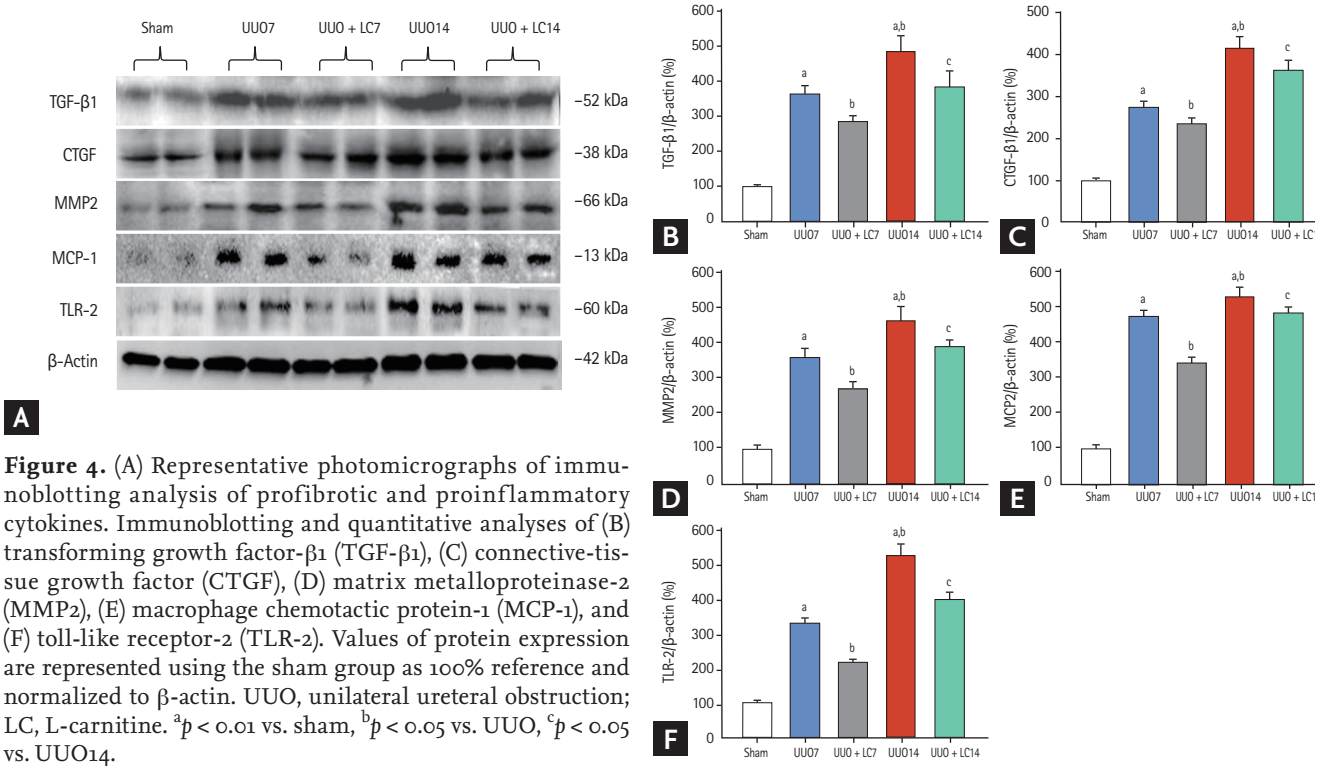

Figure 4. (A) Representative photomicrographs of immunoblotting analysis of profibrotic and proinflammatory cytokines. Immunoblotting and quantitative analyses of (B) transforming growth factor-β1 (TGF-β1), (C) connective-tissue growth factor (CTGF), (D) matrix metalloproteinase-2 (MMP2), (E) macrophage chemotactic protein-1 (MCP-1), and (F) toll-like receptor-2 (TLR-2). Values of protein expression are represented using the sham group as 100% reference and normalized to β-actin. UUO, unilateral ureteral obstruction; LC, L-carnitine. [a]$p < 0.01$ vs. sham, [b]$p < 0.05$ vs. UUO, [c]$p < 0.05$ vs. UUO14.

https://doi.org/10.3904/kjim.2019.413

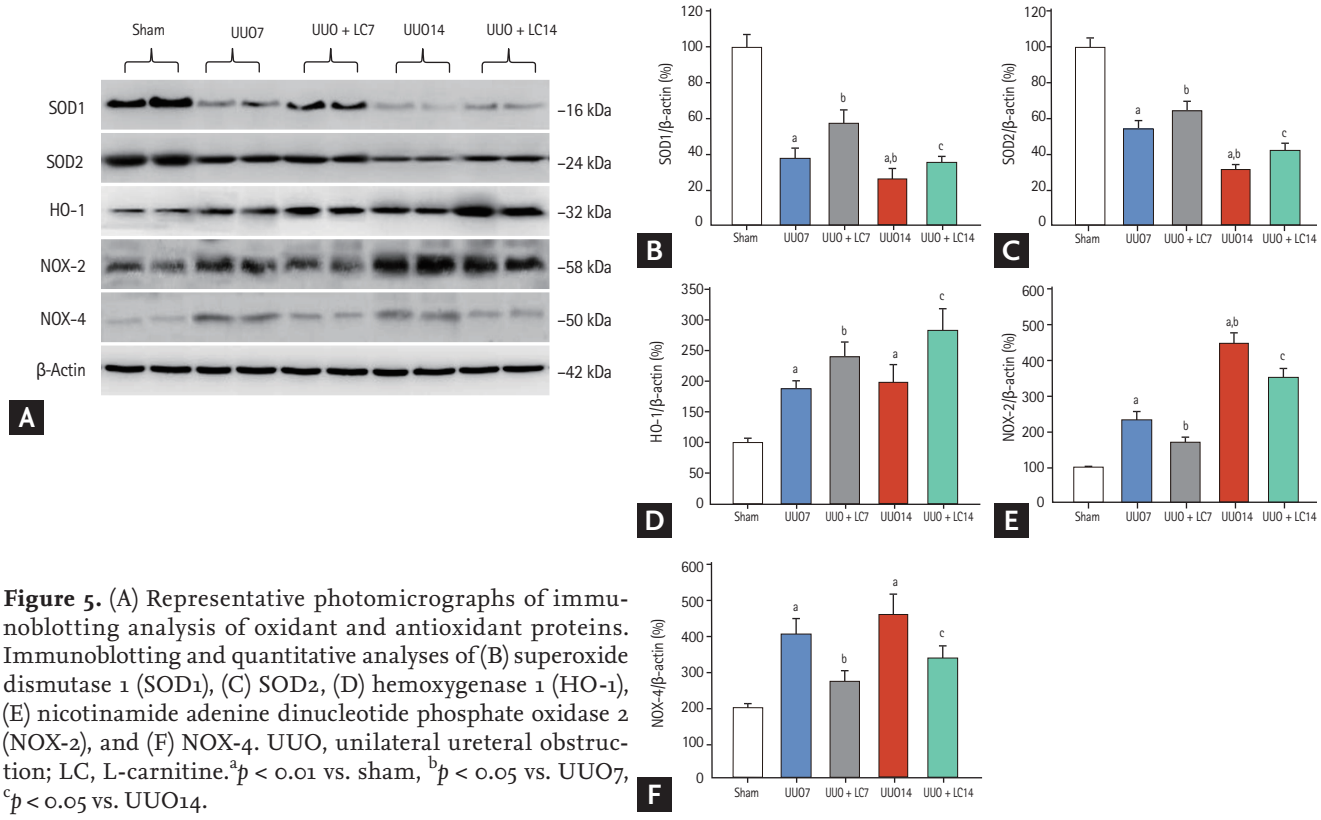

Figure 5. (A) Representative photomicrographs of immunoblotting analysis of oxidant and antioxidant proteins. Immunoblotting and quantitative analyses of (B) superoxide dismutase 1 (SOD1), (C) SOD2, (D) hemoxygenase 1 (HO-1), (E) nicotinamide adenine dinucleotide phosphate oxidase 2 (NOX-2), and (F) NOX-4. UUO, unilateral ureteral obstruction; LC, L-carnitine. [a]$p < 0.01$ vs. sham, [b]$p < 0.05$ vs. UUO7, [c]$p < 0.05$ vs. UUO14.

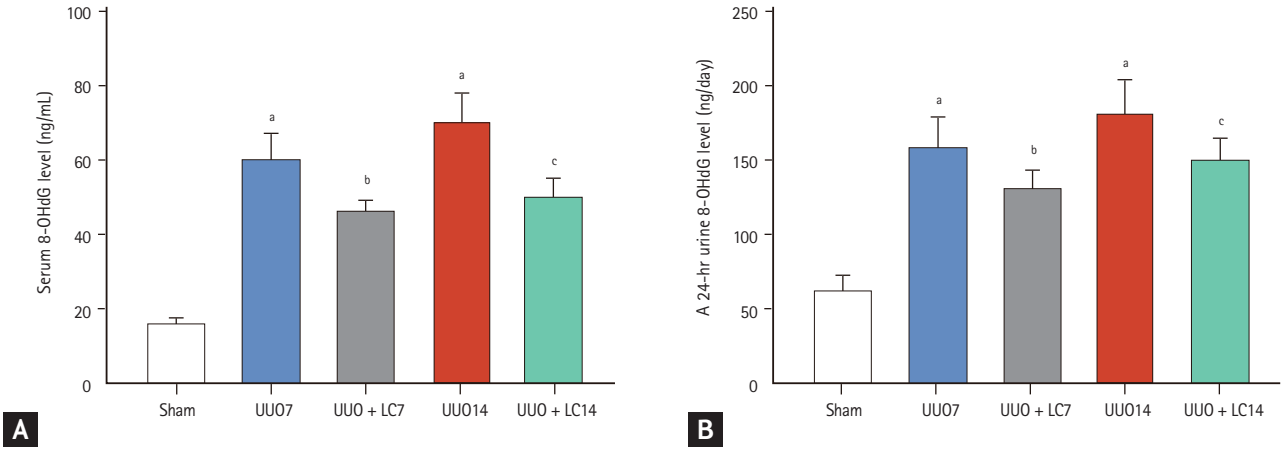

Figure 6. Effect of L-carnitine (LC) on -hydroxy-2′-deoxyguanosine (8-OhdG) concentration in serum (A) and urine (B). UUO, unilateral ureteral obstruction. [a]$p < 0.01$ vs. sham, [b]$p < 0.05$ vs. UUO7, [c]$p < 0.05$ vs. UUO14.

131.54 ± 12.31 ng/day vs. 158.26 ± 21.47 ng/day; UUO14 + LC vs. UUO14: 150.38 ± 14.67 ng/day vs. 181.46 ± 23.37 ng/day, $p < 0.05$, respectively) (Fig. 6B).

LC improves UUO-induced mitochondrial dysfunction

Transmission electron microscopy showed that UUO damaged mitochondrial structures, as indicated by swelling of disorganized cristae, fragmented mitochondria (fission), and mitochondrial fussion (Fig. 3H and 3I).

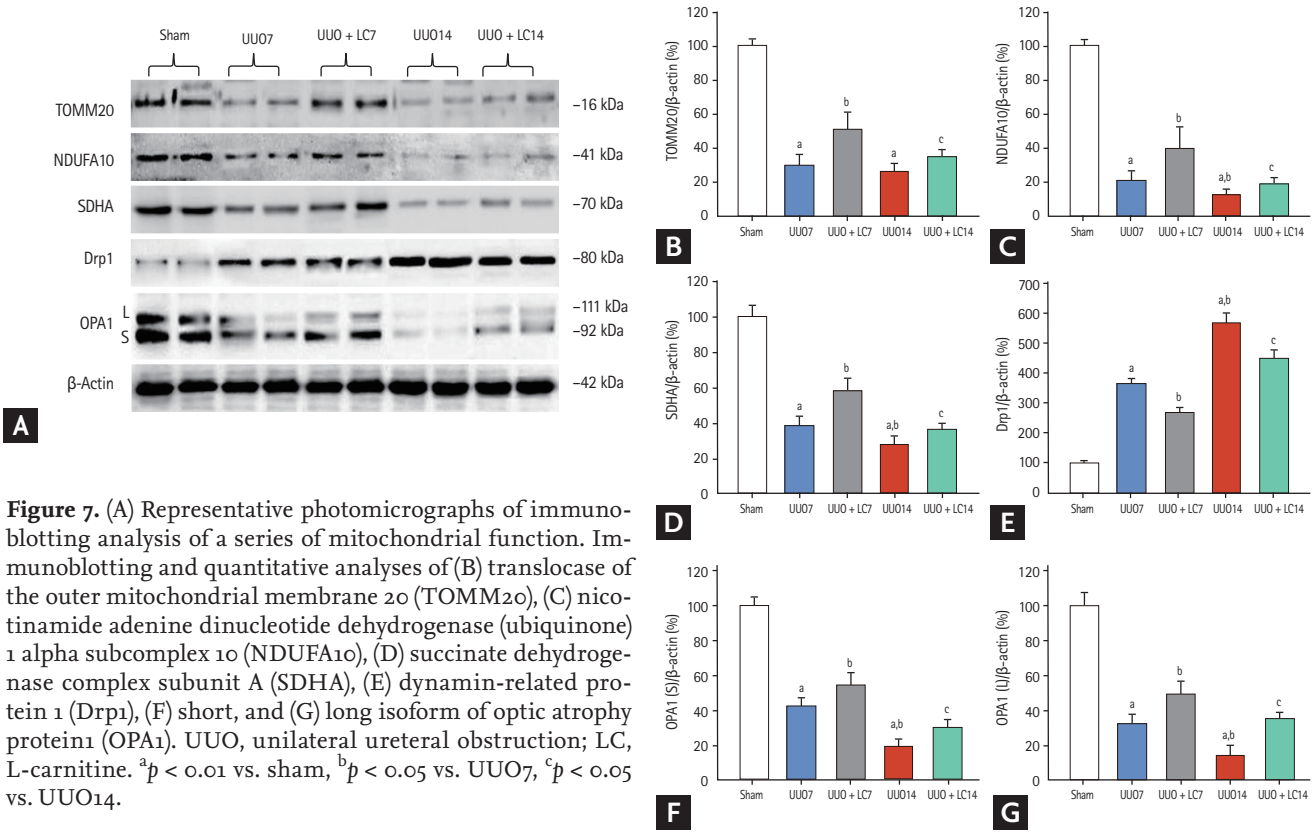

Figure 7. (A) Representative photomicrographs of immunoblotting analysis of a series of mitochondrial function. Immunoblotting and quantitative analyses of (B) translocase of the outer mitochondrial membrane 20 (TOMM20), (C) nicotinamide adenine dinucleotide dehydrogenase (ubiquinone) 1 alpha subcomplex 10 (NDUFA10), (D) succinate dehydrogenase complex subunit A (SDHA), (E) dynamin-related protein 1 (Drp1), (F) short, and (G) long isoform of optic atrophy protein1 (OPA1). UUO, unilateral ureteral obstruction; LC, L-carnitine. $^{a}p < 0.01$ vs. sham, $^{b}p < 0.05$ vs. UUO7, $^{c}p < 0.05$ vs. UUO14.

By our quantitative analysis system, LC treatment preserved the number and size of mitochondrial structure integrity (Fig. 3). Quantitative immunoblotting analysis indicated that expression of TOMM20, NDUFA10 (one of the subunits of complex I), and SDHA was significantly suppressed in obstructed kidneys compared with sham-operated kidneys, whereas the expression of these molecules was restored by treatment with LC (Fig. 7). Moreover, LC decreased expression of Drp1 (fission protein), but increased expression of both the long form and short form of OPA1 (fussion protein). These findings suggest that LC may improve mitochondrial function in rat kidneys after UUO.

LC inhibits UUO-induced programmed cell death

Both of type I (apoptosis) and type II programmed cell death (autophagy) are involved in renal fibrosis of obstructed kidneys. By electron microscopy (Fig. 3E) and TUNEL assay (Fig. 8A), we observed that UUO induced typical apoptotic bodies in renal cells and an increase in the number of TUNEL-positive cells, and this trend was inhibited at both time points by addition of LC. At a molecular level, LC regulated the ratio of expression of Bcl-2 and Bax and suppressed cleaved caspase-3 expression toward levels required for cell survival (Fig. 8B). Additionally, establishment of UUO was associated with excessive autophagy. Using electron microscopy, autophagic components such as lipid droplets, myelinbodies, autolysosomes, and autophagosomes in UUO rat kidneys were observed (Fig. 3G). By immunoblotting analysis, we found that LC decreased expression of autophagy-related genes such as LC3B, Beclin-1, and P62 (Fig. 9). This finding was consistent with our previous data demonstrating the inhibitory effect of LC on autophagy [7].

LC deactivates PI3K/AKT/FoxO1a signaling pathway in UUO

To explore the mechanism of the effect of LC on renal fibrosis after UUO, we evaluated expression of components of the PI3K/AKT/FoxO1a signaling pathway by immunoblotting. As shown in Fig. 10, UUO led to activation of PI3K/AKT/FoxO1a protein expression at days 7 and 14, whereas their expression was inhibited by LC treatment. Our results indicated that LC treatment

https://doi.org/10.3904/kjim.2019.413

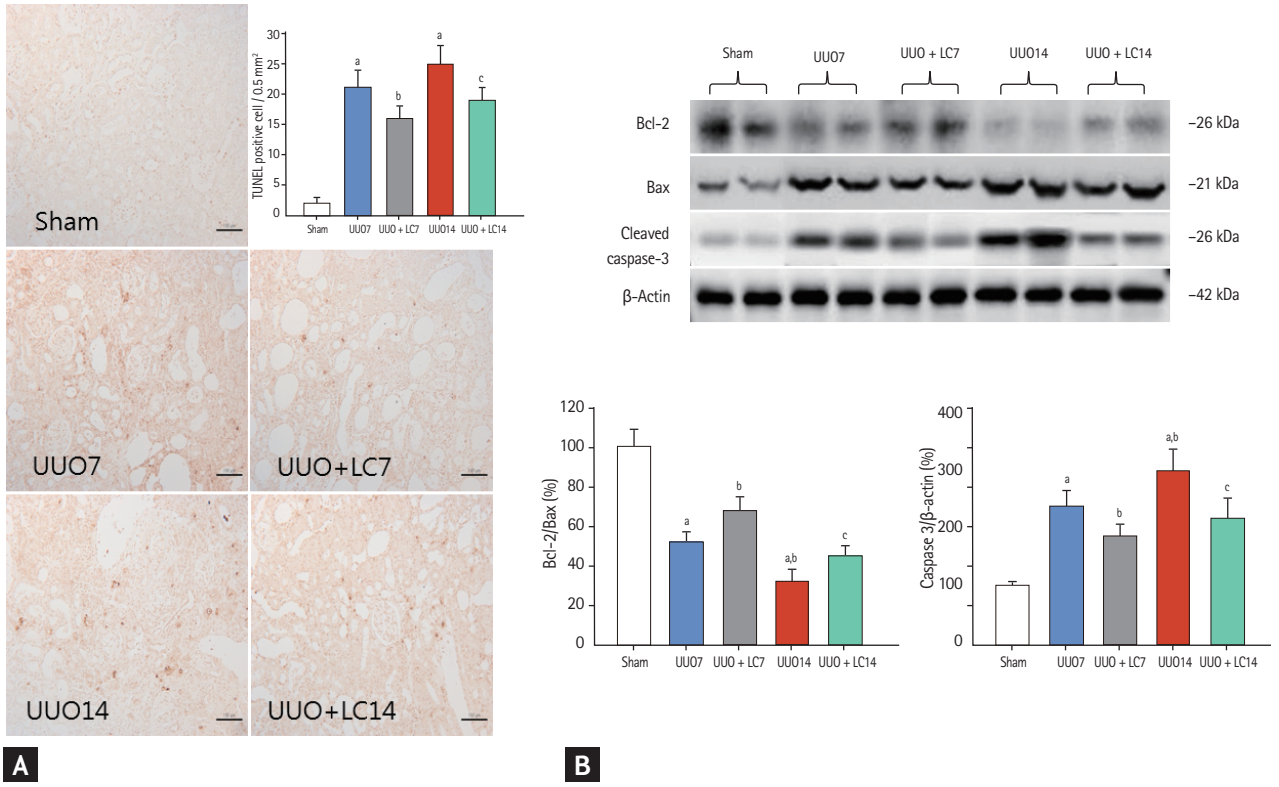

Figure 8. Representative photomicrographs of terminal deoxynucleotidyl transferase dUTP nick end labeling (TUNEL) assay and semiquantitative analysis (A). Immunoblotting and quantitative analyses of Bcl-2, Bax, and cleaved caspase-3 (B). Bcl-2, B-cell lymphoma-2; Bax, Bcl2-associated X; UUO, unilateral ureteral obstruction; LC, L-carnitine. [a]$p < 0.01$ vs. sham, [b]$p < 0.05$ vs. UUO7, [c]$p < 0.05$ vs. UUO14.

attenuates renal fibrosis induced by UUO through the PI3K/AKT/FoxO1a-dependent signaling pathway.

Effect of LC on H_2O_2-treated HK-2 cells

The HK-2 cell line was treated with H_2O_2 to mimic the animal model of UUO-induced hypoxia. Addition of LC inhibited intracellular ROS production (Fig. 11A) and apoptotic cells (Fig. 11B) and dose-dependently improved cell viability in H_2O_2-treated HK-2 cells (Fig. 11C) ($p < 0.001$). Moreover, LC treatment suppressed expression of profibrotic cytokine TGF-β1, CTGF, and α-SMA (Fig. 12). In parallel with our results *in vivo*, this *in vitro* study demonstrated that LC treatment exerts antioxidant effects subsequently inhibit HK-2 cell death.

DISCUSSION

This study clearly demonstrated that LC administration attenuated the progression of TIF in a rat model of UUO by downregulating the expression of proinflammatory and profibrotic cytokines. The effect of LC was associated with lessening oxidative stress, improving mitochondrial function, and modulating programmed cell death via the PI3K/AKT/FoxO1a signaling pathway. *In vitro* experiments demonstrated that LC inhibited ROS production and apoptotic cell death and improved cell viability. Our study illustrated for the first time that LC protects against renal fibrosis of an obstructed kidney.

Inflammation plays a critical role in kidney damage because it precedes renal scarring. The inflammatory response initiates a protective response against injurious stimuli; however, unremitting inflammation drives excessive deposition of extracellular matrix protein in the tubulointerstitial space, leading to irreversible fibrosis. Several proinflammatory and profibrotic cytokines originating from renal tubular epithelial cells, myofibroblasts, and infiltrating macrophages are involved in this process [20]. Of these, macrophages are the major source of fibrosis-associated chemokines and cytokines

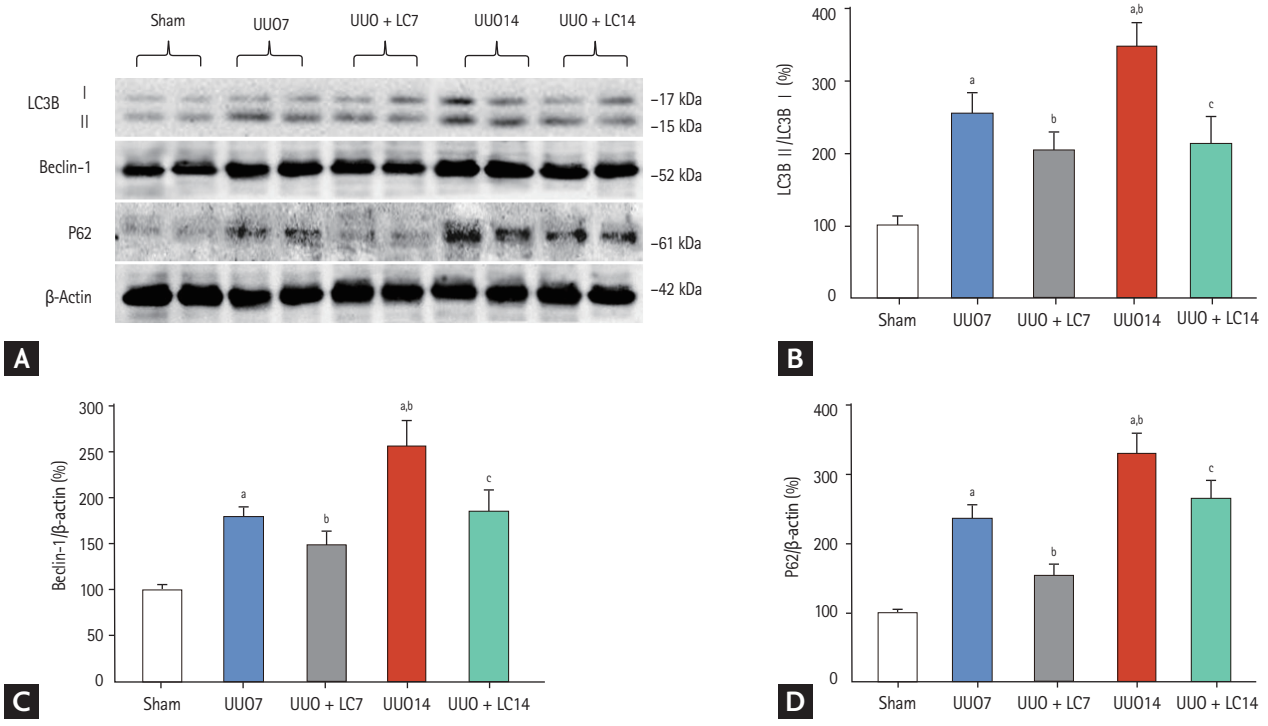

Figure 9. (A) Immunoblotting analysis of autophagy-related genes. Immunoblotting and quantitative analyses of (B) LC3B, (C) beclin-1, and (D) P62. UUO, unilateral ureteral obstruction; LC, L-carnitine; LC3B, light chain 3β. [a]$p < 0.01$ vs. sham, [b]$p < 0.05$ vs. UUO7, [c]$p < 0.05$ vs. UUO14.

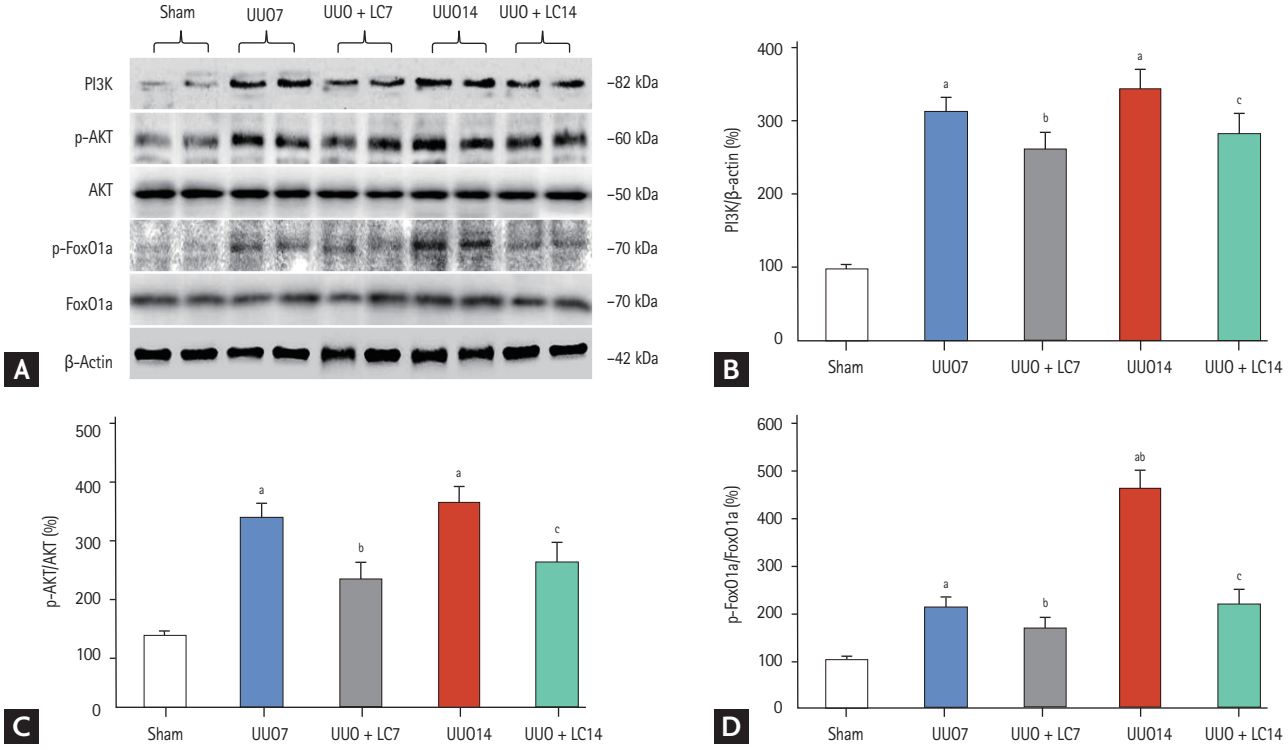

Figure 10. (A) Immunoblotting analysis of components of the phosphatidylinositol 3-kinase (PI3K)/AKT/forkhead box protein O 1a (FoxO1a) signaling pathway. Immunoblotting and quantitative analyses of (B) PI3K, (C) AKT, and (D) FoxO1a. UUO, unilateral ureteral obstruction; LC, L-carnitine. [a]$p < 0.01$ vs. sham, [b]$p < 0.05$ vs. UUO7, [c]$p < 0.05$ vs. UUO14.

https://doi.org/10.3904/kjim.2019.413

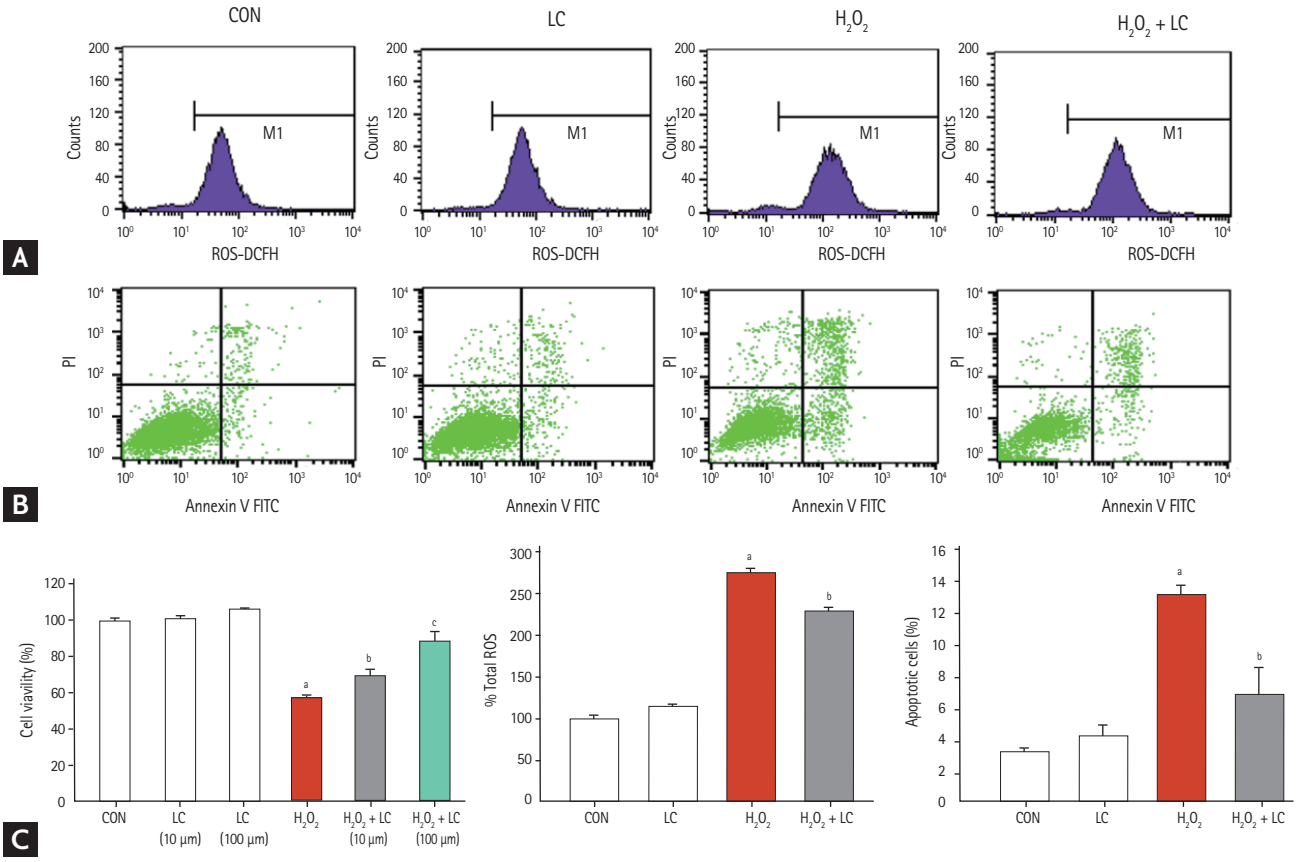

Figure 11. Effect of L-carnitine (LC) on intracellular reactive oxygen species (ROS) production (A), apoptotic cells (B) and cell viability (C) of H_2O_2-treated HK-2 cells. ROS, reactive oxygen species; CON, control; LC, L-carnitine; DCFH, 2',7'-dichlorofluorescin; FITC, fluorescein isothiocyanate. [a]$p < 0.001$ vs. control, [b]$p < 0.05$ vs. H_2O_2, [c]$p < 0.01$ vs. H_2O_2 + LC (10 μM).

such as MCP-1, chemokine receptors, adhesion molecules, and TGF-β1. Chemokines and TGF-β1 in turn recruit inflammatory cells, resulting in a vicious cycle of inflammation. In this study, we found that LC treatment decreased the number of ED-1-positive cells and suppressed expression of the inflammatory mediators OPN, MCP-1, and TLR-2 and the fibrotic cytokines TGF-β1 and CTGF at 7 and 14 days after UUO, and that this was accompanied by a significant attenuation of MMP-2 expression and the severity of TIF. Thus, LC may have anti-inflammatory and antifibrotic effects in this rat model of UUO.

It is unclear how LC abrogates inflammation and fibrosis in this model, but the process may be multifactorial. UUO-induced hypoxia is well known to trigger oxidative stress, which ultimately results in renal inflammation and fibrosis. This concept is supported by studies showing that methionine sulfoxide reductase A deficiency exacerbates the progression of UUO-induced renal fibrosis by upregulating collagen deposition [21], an effect that is alleviated in soluble epoxide hydrolase-knockout mice [22] or by administration of the antioxidant vitamin E [23]. LC directly inhibited NOX-induced oxidative stress and intracellular ROS generation in rat renal epithelial cells (NRK-52E) and in HK-2 cells [24]. We have previously demonstrated that LC decreases intrarenal 8-OHdG expression and thereby protects against cyclosporine-induced renal injury [7]. In the present study, we observed that LC augmented antioxidant protein expression, but decreased oxidant protein expression in obstructed kidneys, thereby minimizing oxidative stress. Moreover, LC suppressed H_2O_2-induced ROS production in HK-2 cell lines. These findings are consistent with previous reports demonstrating the antioxidant capacity of LC in liver [25], heart [26], brain [27], and in diabetes [28], and implying that the

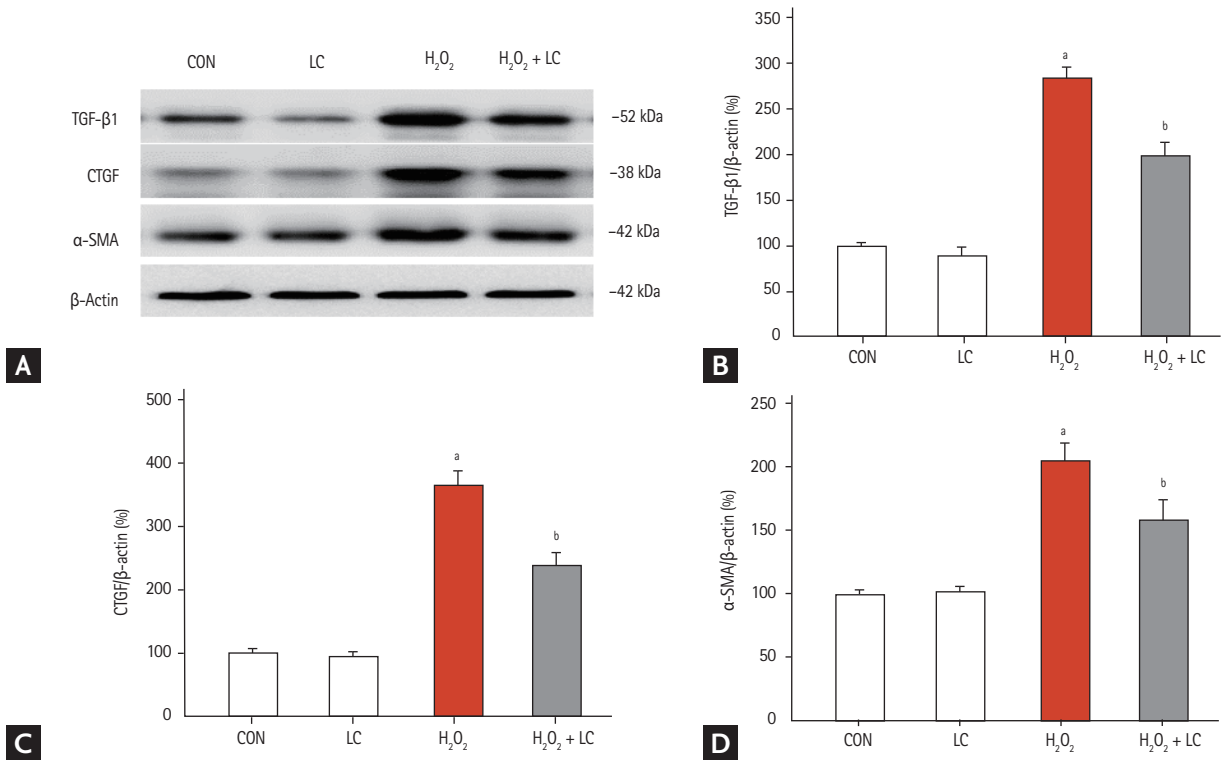

Figure 12. (A) Effect of L-carnitine (LC) on the expression of profibrotic cytokines in H2O2-treated HK-2 cells. Immunoblotting and quantitative analyses of (B) transforming growth factor-β1 (TGF-β1), (C) connective-tissue growth factor (CTGF), and (D) α-smooth muscle actin (α-SMA). CON, control; LC, L-carnitine. [a]$p < 0.001$ vs. control, [b]$p < 0.05$ vs. H_2O_2.

amelioration of tubulointerstitial inflammation and fibrosis by LC in obstructed kidneys may be related to its antioxidant actions.

It is also apparent that LC attenuates renal inflammation and fibrosis through preserving an intact mitochondrial network. The mitochondria are intracellular organelles that play a pivotal role in maintaining cellular energy homeostasis, and are also a major source of ROS. Under pathological conditions, mitochondrial dysfunction can cause inflammation, oxidative damage, and subsequent programmed cell death (apoptosis and autophagy). Therefore, oxidative stress, mitochondrial abnormality, and programmed cell death are interrelated. Previous studies have indicated that LC counteracts age-related alterations in mitochondrial biogenesis and dynamics in the brain of old rats [27] and improves mitochondrial function in mice with high-calorie diet/streptozotocin-induced type 2 diabetes [14]. The results of the present study demonstrated that UUO destroyed mitochondrial architecture and function, that mitochondrial dysfunction was paralleled by excessive apoptosis and autophagy and dysregulation of the expression of a series of genes, and that all these effects were reversed by administering LC. Moreover, LC treatment induced a dose-dependent improvement in the viability of H_2O_2-treated HK-2 cells, and inhibited apoptotic cell death. Taken together, these findings suggest that alleviation of apoptosis and autophagy by LC is closely associated with preservation of the mitochondrial network.

Our results revealed that LC treatment not only markedly reduced the severity of TIF, but also suppressed expression of profibrotic cytokines (e.g., TGF-β1, CTGF, and α-SMA); however, there were no significant differences in renal function among the experimental groups. This unexpected finding was also observed in another study: e.g., Moosavi et al. [29] reported that LC could decrease oxidative stress and suppress energy metabolism but did not improve renal function. A comparison of the two animal models shows that Moosavi et al. [29] used a rat model characterized by the release of obstruction

https://doi.org/10.3904/kjim.2019.413

after 24 hours of UUO induction and a relatively short treatment period (22 hours), whereas our UUO model produced TIF and renal function recovered over 7 to 14 days because of compensatory function from the contralateral kidney [30]. These findings raise the possibility that the effectiveness of LC in UUO is dependent on the period of drug treatment. Our result is consistent with those of previous studies by Shirazi et al. [31] and Moosavi et al. [32] that demonstrated the renoprotective effect of LC on the obstructed kidney.

FoxO transcription factors belong to a family of stress-responsive regulators of various downstream target genes that govern the expression of proteins involved in cellular proliferation, apoptosis, longevity, cancer, antioxidant defense, and regulation of the cell cycle and metabolism [33-35]. The FoxOs are regulated by posttranslational modifications such as phosphorylation, acetylation, and ubiquitination through the PI3K/AKT pathway, and phosphorylation of FoxOs induces inactivation and nuclear exclusion of FoxOs [36]. It has been reported that the activation and subcellular localization of FoxOs are mediated by ROS, and that in turn, FoxOs regulate several antioxidant enzymes such as manganese superoxide dismutase and catalase, thus protecting cells from oxidative stress [37]. As a result, the PI3K/AKT/FoxO1a signaling pathway plays an important role in ROS-associated diseases including CKD. In this study, we found that LC inhibited the expression of PI3K, phosphorylated AKT and phosphorylated FoxO1a in obstructed kidneys, and that this was concomitant with a decrease in oxidative stress. Therefore, it is likely that LC provides antioxidant effects in this model by modulation of the PI3K/AKT/FoxO1a signaling pathway.

In clinical practice, LC supplementation is often used to manage carnitine deficiency caused by genetic disorders, or chronic hemodialysis, or chronic heart failure [38]. However, LC may have diverse uses because it possesses antioxidant activity. For example, administration of LC improves cardiovascular injury in patients on hemodialysis, as well as in myocardial infarction patients with angina pectoris, left-ventricular enlargement or dilation, and arrhythmias. In addition, LC ameliorates hepatic steatosis in nonalcoholic fatty liver disease and diabetes [39]. These benefits are reflected in a variety of animal models [26,40]. Based on our results and previous reports, we propose that treating CKD patients with LC as early as possible may result in additional benefits beyond carnitine supplementation. Future clinical trials are needed to resolve this issue.

In summary, this study showed that LC treatment prevented tubulointerstitial inflammation and fibrosis in a UUO model. Inhibition of oxidative stress and programmed cell death together with an improvement in mitochondrial function via the PI3K/AKT/FoxO1a signaling pathway may be one mechanism underlying the renoprotective effects of LC. This study may provide a rationale for the clinical use of LC in CKD patients.

KEY MESSAGE

1. L-carnitine (LC) treatment prevents renal tubulointerstitial inflammation and fibrosis in rat model of unilateral ureteral obstruction.
2. LC preserves the integrity of mitochondrial network.
3. LC suppresses the programmed cell death.
4. Inhibition of oxidative stress and programmed cell death together with an improvement in mitochondrial function via the PI3K/AKT/FoxO1a signaling pathway may be one mechanism underlying the renoprotective effects of LC.

Conflict of interest

No potential conflict of interest relevant to this article was reported.

Acknowledgments

This study was supported by the National Natural Science Foundation of China (No. 81560125; No.81760293; No.81760132); Science and Technology Research "13th Five-Year Plan" Projects of Education Department of Jilin Province (JJHK20180890KJ; JJHK20180915KJ).

REFERENCES

1. Wong SP, Hebert PL, Laundry RJ, et al. Decisions about renal replacement therapy in patients with advanced kidney disease in the US Department of Veterans Affairs, 2000-2011. Clin J Am Soc Nephrol 2016;11:1825-1833.
2. Wang M, Liu R, Jia X, Mu S, Xie R. N-acetyl-seryl-aspar-

tyl-lysyl-proline attenuates renal inflammation and tubulointerstitial fibrosis in rats. Int J Mol Med 2010;26:795-801.
3. Xu Y, Ruan S, Wu X, Chen H, Zheng K, Fu B. Autophagy and apoptosis in tubular cells following unilateral ureteral obstruction are associated with mitochondrial oxidative stress. Int J Mol Med 2013;31:628-636.
4. Giudetti AM, Stanca E, Siculella L, Gnoni GV, Damiano F. Nutritional and hormonal regulation of citrate and carnitine/acylcarnitine transporters: two mitochondrial carriers involved in fatty acid metabolism. Int J Mol Sci 2016;17:817.
5. Fan JP, Kim D, Kawachi H, Ha TS, Han GD. Ameliorating effects of L-carnitine on diabetic podocyte injury. J Med Food 2010;13:1324-1330.
6. Xue M, Chen X, Guo Z, et al. L-carnitine attenuates cardiac dysfunction by ischemic insults through Akt signaling pathway. Toxicol Sci 2017;160:341-350.
7. Xiang Y, Piao SG, Zou HB, et al. L-carnitine protects against cyclosporine-induced pancreatic and renal injury in rats. Transplant Proc 2013;45:3127-3134.
8. Liu Y, Yan S, Ji C, et al. Metabolomic changes and protective effect of (L)-carnitine in rat kidney ischemia/reperfusion injury. Kidney Blood Press Res 2012;35:373-381.
9. Kunak CS, Ugan RA, Cadirci E, et al. Nephroprotective potential of carnitine against glycerol and contrast-induced kidney injury in rats through modulation of oxidative stress, proinflammatory cytokines, and apoptosis. Br J Radiol 2016;89:20140724.
10. Zambrano S, Blanca AJ, Ruiz-Armenta MV, et al. L-carnitine attenuates the development of kidney fibrosis in hypertensive rats by upregulating PPAR-γ. Am J Hypertens 2014;27:460-470.
11. Gunes D, Kirkim G, Kolatan E, et al. Evaluation of the effect of acetyl L-carnitine on experimental cisplatin ototoxicity and neurotoxicity. Chemotherapy 2011;57:186-194.
12. Boonsanit D, Kanchanapangka S, Buranakarl C. L-carnitine ameliorates doxorubicin-induced nephrotic syndrome in rats. Nephrology (Carlton) 2006;11:313-320.
13. Tsogbadrakh B, Ju KD, Lee J, et al. HL156A, a novel pharmacological agent with potent adenosine-monophosphate-activated protein kinase (AMPK) activator activity ameliorates renal fibrosis in a rat unilateral ureteral obstruction model. PLoS One 2018;13:e0201692.
14. Xia Y, Li Q, Zhong W, Dong J, Wang Z, Wang C. L-carnitine ameliorated fatty liver in high-calorie diet/STZ-induced type 2 diabetic mice by improving mitochondrial function. Diabetol Metab Syndr 2011;3:31.
15. Lim SW, Jin L, Luo K, et al. Klotho enhances FoxO3-mediated manganese superoxide dismutase expression by negatively regulating PI3K/AKT pathway during tacrolimus-induced oxidative stress. Cell Death Dis 2017;8:e2972.
16. Wu M, Li R, Hou Y, et al. Thioredoxin-interacting protein deficiency ameliorates kidney inflammation and fibrosis in mice with unilateral ureteral obstruction. Lab Invest 2018;98:1211-1224.
17. Chung S, Jeong JY, Chang YK, et al. Concomitant inhibition of renin angiotensin system and Toll-like receptor 2 attenuates renal injury in unilateral ureteral obstructed mice. Korean J Intern Med 2016;31:323-334.
18. Chen X, Wei SY, Li JS, et al. Overexpression of heme oxygenase-1 prevents renal interstitial inflammation and fibrosis induced by unilateral ureter obstruction. PLoS One 2016;11:e0147084.
19. Qiao X, Wang L, Wang Y, et al. Intermedin attenuates renal fibrosis by induction of heme oxygenase-1 in rats with unilateral ureteral obstruction. BMC Nephrol 2017;18:232.
20. Ichii O, Kimura J, Okamura T, et al. IL-36α regulates tubulointerstitial inflammation in the mouse kidney. Front Immunol 2017;8:1346.
21. Kim JI, Noh MR, Kim KY, Jang HS, Kim HY, Park KM. Methionine sulfoxide reductase A deficiency exacerbates progression of kidney fibrosis induced by unilateral ureteral obstruction. Free Radic Biol Med 2015;89:201-208.
22. Kim J, Imig JD, Yang J, Hammock BD, Padanilam BJ. Inhibition of soluble epoxide hydrolase prevents renal interstitial fibrosis and inflammation. Am J Physiol Renal Physiol 2014;307:F971-F980.
23. Kuemmerle NB, Brandt RB, Chan W, Krieg RJ Jr, Chan JC. Inhibition of transforming growth factor beta 1 induction by dietary vitamin E in unilateral ureteral obstruction in rats. Biochem Mol Med 1997;61:82-86.
24. Ye J, Li J, Yu Y, Wei Q, Deng W, Yu L. L-carnitine attenuates oxidant injury in HK-2 cells via ROS-mitochondria pathway. Regul Pept 2010;161:58-66.
25. Abu-El-Zahab HSH, Hamza RZ, Montaser MM, El-Mahdi MM, Al-Harthi WA. Antioxidant, antiapoptotic, antigenotoxic, and hepatic ameliorative effects of L-carnitine and selenium on cadmium-induced hepatotoxicity and alterations in liver cell structure in male mice. Ecotoxicol Environ Saf 2019;173:419-428.
26. Vacante F, Senesi P, Montesano A, Frigerio A, Luzi L, Ter-

https://doi.org/10.3904/kjim.2019.413

ruzzi I. L-carnitine: an antioxidant remedy for the survival of cardiomyocytes under hyperglycemic condition. J Diabetes Res 2018;2018:4028297.
27. Nicassio L, Fracasso F, Sirago G, et al. Dietary supplementation with acetyl-L-carnitine counteracts age-related alterations of mitochondrial biogenesis, dynamics and antioxidant defenses in brain of old rats. Exp Gerontol 2017;98:99-109.
28. Rezaei N, Mardanshahi T, Shafaroudi MM, Abedian S, Mohammadi H, Zare Z. Effects of L-carnitine on the follicle-stimulating hormone, luteinizing hormone, testosterone, and testicular tissue oxidative stress levels in streptozotocin-induced diabetic rats. J Evid Based Integr Med 2018;23:2515690X18796053.
29. Moosavi SM, Ashtiyani SC, Hosseinkhani S. L-carnitine improves oxidative stress and suppressed energy metabolism but not renal dysfunction following release of acute unilateral ureteral obstruction in rat. Neurourol Urodyn 2011;30:480-487.
30. Zhang QF. Ulinastatin inhibits renal tubular epithelial apoptosis and interstitial fibrosis in rats with unilateral ureteral obstruction. Mol Med Rep 2017;16:8916-8922.
31. Shirazi M, Noorafshan A, Kroup M, Tanideh N. Comparison of the effects of captopril, tamoxifen and L-carnitine on renal structure and fibrosis after total unilateral ureteral obstruction in the rat. Scand J Urol Nephrol 2007;41:91-97.
32. Moosavi SM, Ashtiyani SC, Hosseinkhani S, Shirazi M. Comparison of the effects of L-carnitine and alpha-tocopherol on acute ureteral obstruction-induced renal oxidative imbalance and altered energy metabolism in rats. Urol Res 2010;38:187-194.
33. Essers MA, de Vries-Smits LM, Barker N, Polderman PE, Burgering BM, Korswagen HC. Functional interaction between beta-catenin and FOXO in oxidative stress signaling. Science 2005;308:1181-1184.
34. Zhang X, Tang N, Hadden TJ, Rishi AK. Akt, FoxO and regulation of apoptosis. Biochim Biophys Acta 2011;1813:1978-1986.
35. Bartholome A, Kampkotter A, Tanner S, Sies H, Klotz LO. Epigallocatechin gallate-induced modulation of FoxO signaling in mammalian cells and C. elegans: FoxO stimulation is masked via PI3K/Akt activation by hydrogen peroxide formed in cell culture. Arch Biochem Biophys 2010;501:58-64.
36. Maiese K, Chong ZZ, Shang YC, Hou J. A "FOXO" in sight: targeting Foxo proteins from conception to cancer. Med Res Rev 2009;29:395-418.
37. Kops GJ, Dansen TB, Polderman PE, et al. Forkhead transcription factor FOXO3a protects quiescent cells from oxidative stress. Nature 2002;419:316-321.
38. Song X, Qu H, Yang Z, Rong J, Cai W, Zhou H. Efficacy and safety of L-carnitine treatment for chronic heart failure: a meta-analysis of randomized controlled trials. Biomed Res Int 2017;2017:6274854.
39. Bae JC, Lee WY, Yoon KH, et al. Improvement of nonalcoholic fatty liver disease with carnitine-orotate complex in type 2 diabetes (CORONA): a randomized controlled trial. Diabetes Care 2015;38:1245-1252.
40. Tousson E, Hafez E, Zaki S, Gad A. The cardioprotective effects of L-carnitine on rat cardiac injury, apoptosis, and oxidative stress caused by amethopterin. Environ Sci Pollut Res Int 2016;23:20600-20608.